

IN FLIGHT CALIBRATION OF SEVIRI SOLAR CHANNELS ON BOARD MSG PLATFORMS

Dominique Jolivet(1), Jean-Marc Nicolas(2), Emilien Bernard(1), Pierre-Yves Deschamps and Didier Ramon(1)

(1) HYGEOS, Euratechnologies, 165 Avenue de Bretagne, 59000 Lille, France

(2) ICARE CGTD, Université de Lille, Cité Scientifique, Polytech'Lille, 59655 Villeneuve d'Ascq Cedex, France

Abstract

Radiometric calibration method based on Rayleigh scattering over black target has been applied to the solar channel VIS06 (centered at 635nm) of SEVIRI on board MSG-1. In a first step, the error analysis budget is established. Results on data from two months of 2006 show that SEVIRI VIS06 band measurement tends on average to underestimate signal of 6%. Effect of wind speed on calibration factor retrieval is about 2%. Finally, this method has also been tested for large viewing angle to test the plane parallel assumption commonly used in radiative transfer calculation and investigate the potential use of large airmass observation.

1. Description of the method

This method has been initially developed by Hagolle et al. (1999) for POLDER in-flight calibration. The method is based on the use of the atmospheric Rayleigh scattering by molecules which can be exactly calculated for any wavelength and sun-view geometry. To be accurate this method requires that the Rayleigh scattering is the most important contribution of the signal measured at the top of the atmosphere. It requires thus dark surfaces as open ocean. Assuming the wind-speed and the marine reflectance, the only unknown at 635nm is the aerosol scattering contribution which is derived from the VIS08 (centered at 810nm) channel.

In the VIS06 band, the normalized radiance, also called reflectance in this paper, can be expressed as follows :

$$R(\text{VIS06}) = [R_{\text{ray}}(\text{VIS06}) + R_{\text{aer}}(\text{VIS06}) + R_{\text{gli}}(\text{VIS06}) + R_{\text{w}}(\text{VIS06})] \cdot T_{\text{gas}} \quad (1)$$

R_{ray} accounts for the Rayleigh scattering, R_{aer} is the aerosol scattering which depends only on the aerosol optical thickness, AOT, for a fixed model, R_{gli} is the sun-glint reflection depending on wind speed using Cox and Munk (1954) rough sea surface model, R_{w} is the water leaving reflectance (under surface scattering contribution) and T_{gas} is the gaseous transmission factor.

In practice, AOT is retrieved by comparing measurements at 810nm with Look-up tables composed of pre-calculated top of the atmosphere reflectances computed with the Successive Order of Scattering (SOS) radiative transfer code (Deuzé et al., 1989; Lenoble et al. 2007) for AOT values from 0 to 0.2 with a step of 0.02. The estimated signal at 635nm is then derived from similar look-up tables using the retrieved AOT.

Finally the calibration factor, A_k , is defined as the ratio of the estimated reflectance over the measured one :

$$A_k = R_{\text{estimated}}(635) / R_{\text{measured}}(635) \quad (2)$$

2. Error analysis budget

2.1. Rayleigh scattering calculation

The Rayleigh optical thickness is estimated for a standard surface pressure of 1013 hPa. Integrated over the spectral response of the filter, the Rayleigh optical thickness is respectively 0.0533 and 0.0204 in the VIS06 and VIS08 band.

In our algorithm, meteorological data are not used and the choice of the assumed value of the pressure at sea level can lead to errors. For example, a 10 hPa uncertainty on pressure can lead to a 1% uncertainty on the TOA reflectances, i.e., 1% on the calibration factor A_k .

2.2. Gaseous absorption

Table 1 summarizes the main absorbing gases and the gaseous transmittances in the two solar bands. These values have been calculated using 6s (Vermotte et al, 1999) The transmittance depends strongly on the airmass and the gas amount. In a plane-parallel atmosphere the airmass m^* is expressed as :

$$m^* = 1/\cos(\text{SZA}) + 1/\cos(\text{VZA}) \quad [3]$$

where SZA is the solar zenith angle and VZA is the viewing zenith angle.

Channel [minimum – maximum wavelength]	Absorbing Gas (amount)	Transmittance		
		SZA=0 VZA=0 $m^* = 2.00$	SZA=30 VZA=30 $m^* = 2.31$	SZA=60 VZA=60 $m^* = 4.00$
VIS06 [560 – 710 nm]	O ₃ (0.319 cm.atm)	T _{O₃} =0.946	T _{O₃} =0.938	T _{O₃} =0.896
	H ₂ O (23.9 kg/m ²)	T _{H₂O} =0.988	T _{H₂O} =0.987	T _{H₂O} =0.979
VIS08 [740 – 880 nm]	H ₂ O	T _{H₂O} =0.892	T _{H₂O} =0.884	T _{H₂O} =0.845

Table 1 :Value of gaseous transmittance in band VIS06 and VIS08 for different sun-view geometries. These values have been computed with 6s code using a mid-latitude summer atmospheric profile.

Amount of precipitable water are re-analyzed data from the National Center for Environmental Prediction (NCEP) of the National Oceanic and Atmospheric Administration (NOAA). Data are given at 6 hours frequency and at 2.5 degrees spatial resolution (<http://www.cdc.noaa.gov/cdc/>). Ozone data are daily products from Aqua/AIRS

An uncertainty of 5% in the ozone amount leads to uncertainties of about 0.5% on A_k . Uncertainty on water vapor content will have a small direct impact on VIS06 channel and a second smaller indirect impact due to aerosol retrieval using VIS08 channel.

2.3. Aerosols

Aerosol contribution is retrieved using only the VIS08 channel and then the aerosol model must be fixed. We selected a maritime model with 99% (called M99) of relative humidity from Shettle and Fenn (1979). Such a choice can lead to systematic errors in the retrieval of the Aerosol Optical Thickness, AOT, in the VIS08 channel and then in the derivation of the aerosol signal in the VIS06 channel. However, for low aerosol load this error is minimal. Nicolas et al (2006) shows that model variability can cause a maximal error of 1% in the determination of the A_k for AOT, defined at 635nm, less than 0.08.

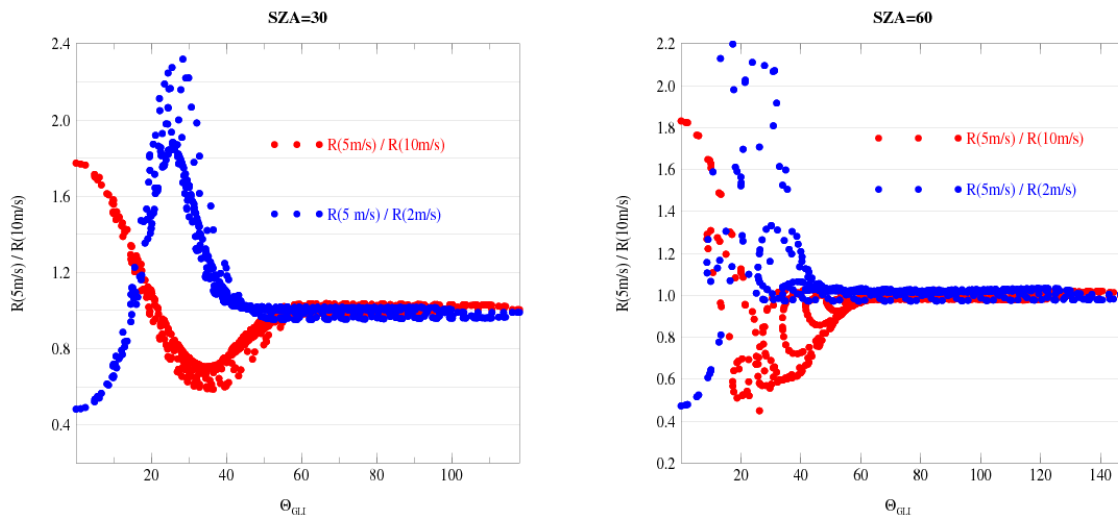
2.4. Marine reflectance

For open ocean (case 1 water), far away from the coastal areas and non eutrophic waters, marine reflectance is small and almost constant in the VIS06 channel. The surface can be assumed completely black in the VIS08 channel. For this study, we assume a chlorophyll concentration of 0.07 mg/m³ which corresponds, following bio-optical model of Morel (1988) and Morel and Maritorena (2001) to a marine reflectance in VIS06 band of 0.0008.

2.5. Wind speed

The surface roughness depends strongly of the wind speed. In this study wind speed is not known from ancillary data. Three values of wind speed have been taken : 2, 5 and 10 m/s. These values are good averages for the three areas selected (see below, section 3) even if large variation can occur.

Figures 1.a and b shows how the reflectances differ in case of wind speed error as a function of the angle between the specular direction and the viewing direction (called Θ_{gli}) for two solar angles. The error is very important, i.e. more than 10%, for Θ_{gli} less than 40 degrees. For errors less than 2%, a threshold of 60 degrees is needed for Θ_{gli} .



(a) (b)
Figure 1 : Ratio of the TOA reflectance at 635nm calculated for 2 different wind speed in case of a molecular atmosphere above a sea rough surface for a solar angle of 30 (a) and 60 degrees (b). The reflectances have been calculated with the SOS radiative transfer code.

2.6. Pixels selection

First of all, cloudy pixels must be discarded. A simple cloud mask based on spectral threshold is used. Moreover, a local standard deviation threshold on VIS08 measurements (made on a 3x3 pixels square) is used to remove neighbored cloudy pixels and remaining clouds. The threshold is 0.005. To ensure low aerosol loads a threshold of 0.05 on the value of the inverted AOT (defined at 635nm) is applied. We only kept measurements made for reasonably high solar elevation (i.e. SZA less than 60 degrees) to optimize signal dynamic resulting from sufficiently large incoming radiation. Finally, sun-glint contaminated pixels are removed using threshold of 60 degrees on the angle between the specular and the viewing direction.

3. Areas selection

The three areas selected are shown in Figure 2. They first have been chosen because of low AOT given by climatology. And they also have been selected to cover different viewing geometry. The area in South Atlantic gives access to VZA between 14 and 31 degrees and thus low airmass. The area in North Atlantic is for VZA between 53 and 70 degrees.. And the area in the North-East of Madagascar allows us to cover very large airmass with a VZA between 65 and 86 degrees.

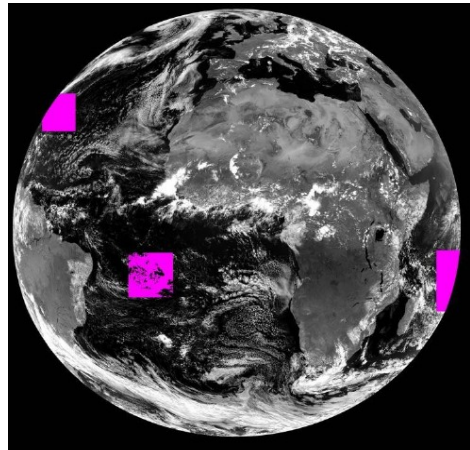


Figure 2 : Areas selected for this study are in magenta in this image in VIS08 band of MSG1/SEVIRI

4. Results

In this section, only pixels with a viewing zenith angle smaller than 60 degrees are kept in order to avoid effect of the Earth curvature. Table 2 summarizes the mean calibration factor A_k retrieved for the area in South Atlantic and North Atlantic, for the month of July and March 2006 assuming three different values of the wind speed. We remark that the retrieved A_k decreases with the wind speed value. Between 2 and 10 m/s A_k varies of about 2%. Results for South Atlantic in March 2006 are sensibly smaller than for the other cases but are within the error budget.

Averaging all these results can give a value of the calibration factor of 0.94, i.e., an underestimation of the signal of $6.0\% \pm 3\%$. It is very closed to the value of 5% found by Nicolas et al. (2006) with the same method and using wind speed data from ECMWF.

Area	Month	Wind speed	Number of pixels	$\langle A_k \rangle$	σ
South Atlantic	July	2	151 328	0.950	0.032
		5	195 844	0.944	0.032
		10	97 959	0.931	0.029
North Atlantic	July	2	35 504	0.946	0.023
		5	45 496	0.941	0.022
		10	60 374	0.937	0.022
South Atlantic	March	2	291 474	0.927	0.035
		5	316 499	0.924	0.034
		10	189 666	0.918	0.023
North Atlantic	March	2	17 522	0.941	0.019
		5	24 416	0.935	0.019
		10	33 334	0.931	0.019

Table 2 : Mean value of the calibration factor A_k , standard deviation, and number of pixels used in the statistics for the areas in South Atlantic and North Atlantic for July and March 2006. Three different values of the wind speed have been assumed.

5. Application to large airmass – Effect of Earth curvature

In this section, we applied the Rayleigh calibration method to large viewing angles. Large viewing angles ensure us large airmass and thus the atmospheric signal is maximized comparing to the surface contribution.

Figure 4 shows the value of the mean calibration factor A_k versus the viewing zenith angle for the area in the North East of Madagascar in March 2006. We first remark that the value of A_k is significantly smaller than the values retrieved in section 4. The wind speed uncertainty can not explain these small values. Moreover, the A_k tends to decrease with the VZA. The first explanation of such results is the effect of the Earth curvature on calculation of the gaseous transmittance and the scattering radiative transfer.

For large sun-view geometries the plane-parallel assumption, commonly used in radiative transfer calculation, is not valid anymore.

The definition of the airmass m^* will be affected taking into account the spherical geometry of the Earth-Atmosphere system. In order to estimate this impact on the computation of the transmittance we focus only on the ozone layer absorbing in VIS06 channel. On a first order approximation, we can model the ozone atmospheric layer as a homogeneous layer located between 20 and 40 km height. In this case, the airmass, in spherical geometry, is smaller than the plane-parallel airmass. Thus it leads to greater transmittance as seen in Figure 5 for a sun at the zenith (SZA = 0 degree). Effect will consequently increase with SZA. The spherical geometry must be taking into account for large airmass because it can lead to error on A_k greater than 1% for viewing angle greater than 78 degrees.

Due to the importance of the geometrical effect, more investigation has to be done to obtain accurate transmittance for more realistic vertical profile of ozone. However, the simple vertical model used in this study allows us a simple correction which can be seen as a first order correction.

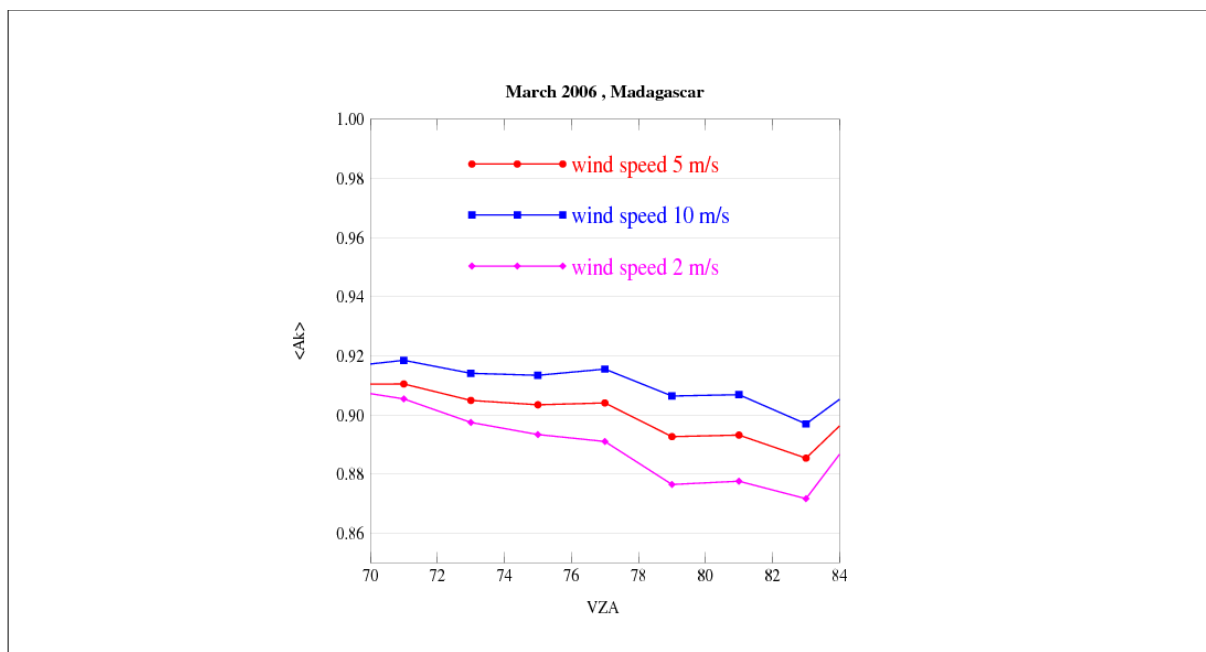
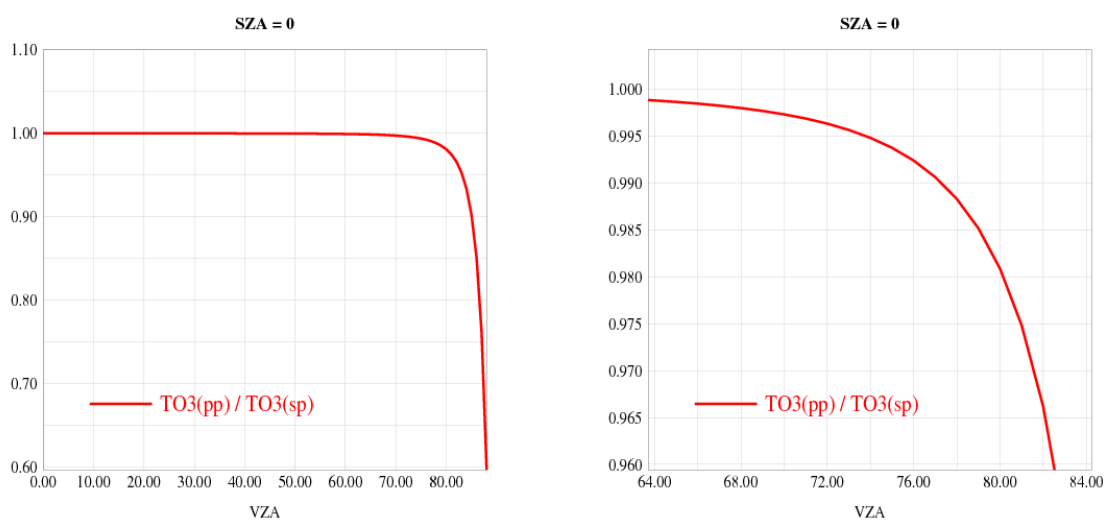


Figure 4 : Average value of the calibration factor A_k versus the viewing zenith angle for the area near Madagascar in July 2006.



a

b

Figure 5 : Ratio of the value of the ozone transmittance in plane-parallel geometry over the value calculated taking into account spherical geometry as a function of the viewing zenith angle (a). On the right (b) we made a zoom for large value of the VZA

The impact of the plane-parallel assumption can also be identified for scattering process. To take into account the spherical geometry we used a Monte Carlo radiative transfer code. The relative difference between the reflectance with or without plane-parallel assumption is shown in Figure 6 for a molecular atmosphere over a rough surface with a wind speed of 5 m/s. The molecules are vertically distributed following an exponential law with a scale height of 8km and the top of the atmosphere is at 100km. For VZA of 70° and moderate SZA the plane parallel assumption tends to overestimate the reflectance of 2%. The difference increases with the VZA. For solar angle between zenith and 40 degrees, the relative difference is between 2 and 8 % for VZA between 70 and 85 degrees.

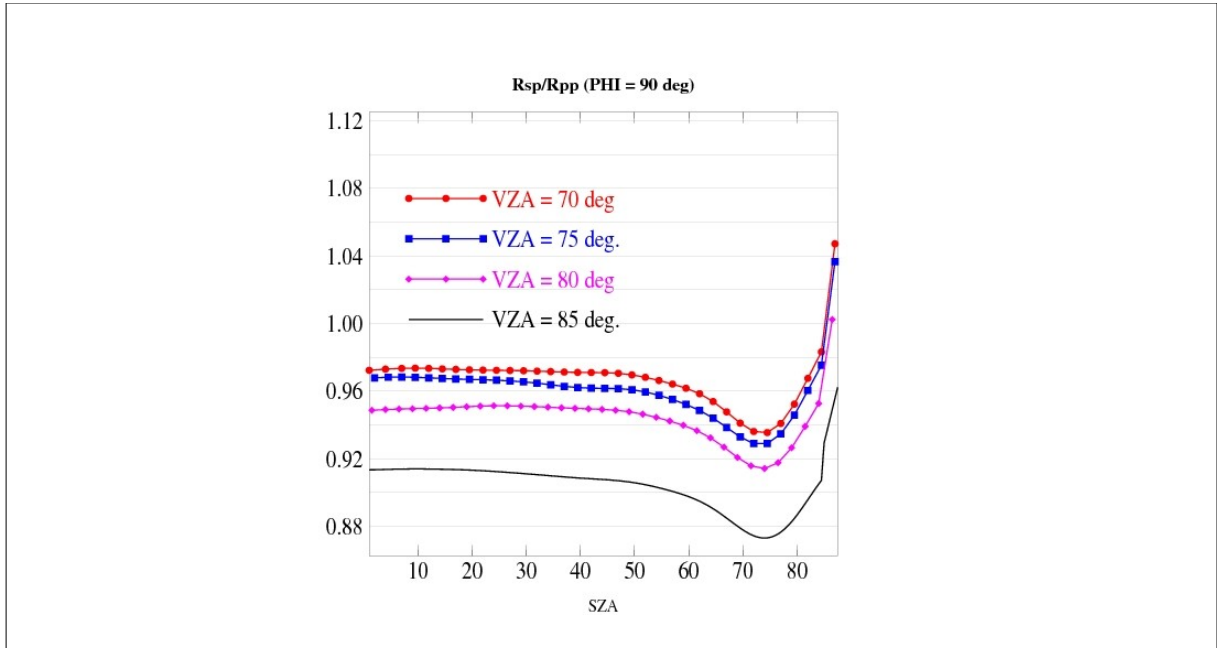


Figure 6 : Ratio of the TOA reflectance at 635nm calculated in spherical geometry over the reflectance calculated in a plane-parallel atmosphere as a function of the solar zenith angle for different values of the viewing zenith angle. The relative azimuth angle is 90 degrees. The atmosphere is only composed of molecules. The wind speed is 5 m/s. For reason of consistency, both plane parallel and spherical calculations have been performed with the Monte Carlo radiative transfer code.

The effect of the Earth curvature for moderate SZA and large VZA leads then to an over estimation of the calculated reflectance using plane parallel assumption. It explain thus why we obtained smaller Ak (measured reflectance over estimated reflectance) for these geometries.

After correcting from Earth curvature by multiplying the Ak factor by the ratio of the transmittances (as defined in figure 5) and the ratio of reflectances obtained in plane-parallel and spherical geometry (as in Figure 6), we can calculate a new calibration Ak (see Figure 6).

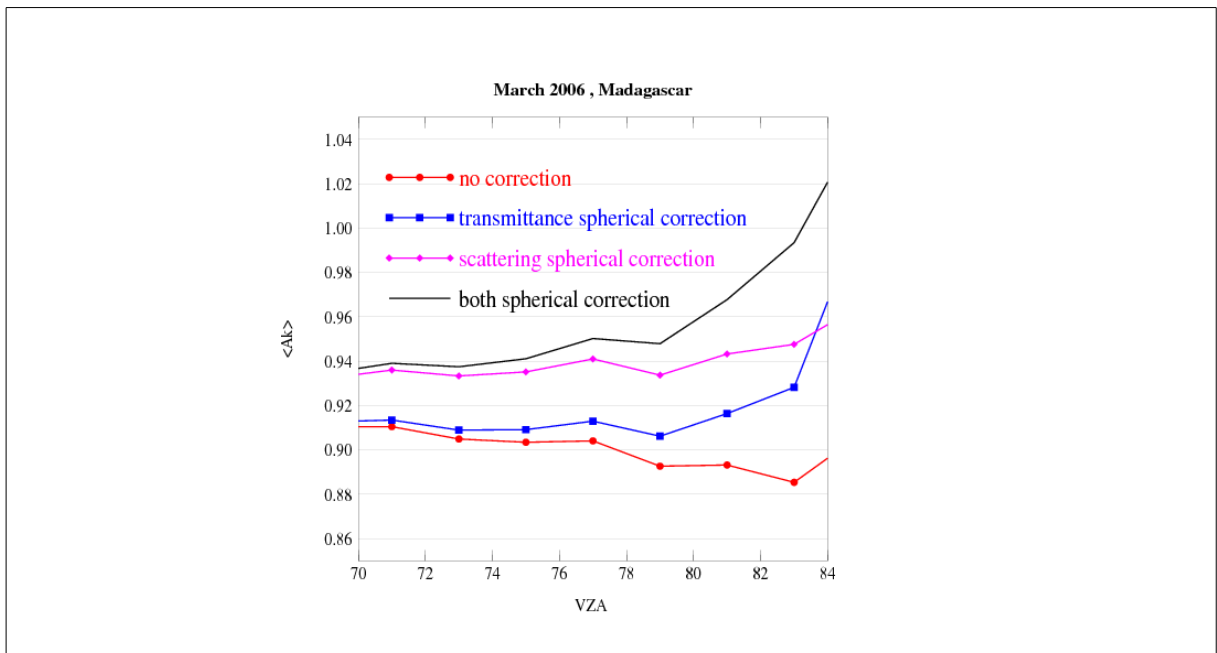


Figure 6 : Mean value of the calibration factor Ak versus the viewing zenith angle for the area near Madagascar in March 2006 before and after correction of Earth curvature

We first remark that the scattering spherical correction alone seems to be enough to find expected A_k (around 0.94) non dependent of the VZA. Adding the transmittance correction, the resulting calibration factor is about 0.94 (6%) for VZA less than 80° . This result is closed to those obtained for moderate and usual viewing angles. But after 80 degrees, the calibration factor increases significantly. It can be due to the simple assumption we made on the vertical profile of the ozone layer. The impact of Earth curvature is very strong on absorption for very large angle. Firstly, we may investigate deeper this impact with realistic vertical profile because it clearly seems we over-corrected with our simple homogeneous layer model. Secondly we must study the absorption-scattering coupling for large airmass and test the validity of the assumptions made in transmittance calculation. Finally, for the scattering processes in spherical geometry, Monte Carlo calculations are very time consuming. In the near future, aerosols must be included in these calculations. The best will be to use pre-calculated radiances and Look-up-tables using the spherical Monte Carlo code.

However, at this stage of this study, we show it is possible to work in extreme geometries and large airmass.

6. Conclusions

A calibration method based on Rayleigh calculation over black targets in the ocean has been applied to solar measurements of MSG-1/SEVIRI in VIS06 band. For moderate airmass and thus for the low part of the signal dynamic, we found that MSG-1/SEVIRI measurements tends to underestimate the signal of about 6%. To better define the calibration factor and obtain an accuracy better than 2%, the wind speed must be known.

We also applied this vicarious calibration method to large airmass and very large viewing angle greater than 70° . Taken into account Earth curvature using Monte Carlo calculation and simple geometrical parameterization of the atmosphere for the gaseous transmittance estimation, we show that we are able to find similar values of the calibration factor. It allows then to work with measurements made in extreme geometries using adapted and realistic transmittance model and radiative transfer code.

Acknowledgments

This study has been partly sponsored by the Centre National d'Etudes Spatiales (CNES, France) under contract 45000024514/DCT094. The authors want also especially thank Bertrand Fougne from CNES for rich discussions and helpful remarks.

References

- Cox, C. and W. Munk, 1954: Measurements of the roughness of the sea surface from photographs of the sun's glitter, *J. Opt. Soc. Am.*, **44**, 11, 838-850.
- Deuzé J.-L., M. Herman, and R. Santer, 1989: Fourier series expansion of the transfer equation in the atmosphere-ocean system. *J. Quant. Spectro. Radiat. Transfer*, vol. **41**, 6, 483-494.
- Hagolle, O, et al., 1999: Results of POLDER In-Flight calibration, *IEEE Trans. Geosci. Remote Sensing*, vol. **37**, 1550-1566.
- Lenoble, J., M. Herman, J.L. Deuzé,, B. Lafrance, R. Santer, D. Tanré, 2007: A successive order of scattering code for solving the vector equation of transfer in the earths atmosphere with aerosols *Journal of Quantitative Spectroscopy & Radiative Transfer*, 107 (2007) 479507 doi:10.1016/j.jqsrt.2007.03.010
- Morel, A., 1988: Optical modeling of the upper ocean in relation to its biogenous matter content (case 1 water), *Journal of Geophysical Research*, **93**, 10,749-10,768
- Morel, A., and S. Maritorena, 2001: Bio-optical properties of oceanic waters: A reappraisal. *Journal of Geophysical research*, **106**, 7763-7780
- Nicolas J.-M., P.-Y. Deschamps and O. Hagolle, 2006: Radiometric Calibration of the Visible and Near-Infrared Bands of SevirI Using Rayleigh Scattering and Sun-Glint Over Oceans. *Proceedings of the 3rd MSG RAO Workshop (ESA SP-619)*. 15 June 2006, Helsinki, Finland. Editor: D. Danessy, p.19
- Shettle, E. P. and R. W. Fenn, 1979: Models of the Aerosols of the Lower Atmosphere and the Effects of Humidity Variations on their Optical Properties. *Project 7670*, Air Force Geoph. Lab., Massachusetts.

Vermote, E, D. Tanré, J.-L. Deuzé, M. Herman and J.-J. Morcrette, 1999: Second simulation of the satellite signal in the solar spectrum, 6s : an overview, *IEEE Trans. Geosci. Remote Sensing*, vol. **35**, 675-686